MEASUREMENT OF THE $t\bar{t}\gamma$ PRODUCTION CROSS SECTION IN PROTON–PROTON COLLISIONS AT $\sqrt{s} = 8$ TeV WITH THE ATLAS DETECTOR*

Sara Ghasemi

on behalf of the ATLAS Collaboration

University of Siegen, Siegen, Germany

(Received April 26, 2018)

The cross section of top-quark pair production in association with a photon in proton–proton collisions at a center-of-mass energy of $\sqrt{s} = 8$ TeV is measured. The data with a total integrated luminosity of 20.2 fb^{-1} collected by the ATLAS detector at the Large Hadron Collider in 2012 is used. The measurement is performed in the single lepton decay channel. The signal region is defined by the final state of exactly one high-p_{T} lepton, large missing transverse momentum, at least four jets where at least one is being b-tagged and exactly one photon with $p_{\mathrm{T}} > 15$ GeV. The cross section times the branching ratio is determined in a fiducial region defined in terms of the detector acceptance. In addition, the first differential cross-section measurements as a function of photon p_{T} and η are presented. The measured fiducial inclusive and differential cross sections are in a good agreement with the next-to-leading order (NLO) prediction.

DOI:10.5506/APhysPolB.49.1127

1. Introduction

The cross-section measurement of top-quark pair production in association with a photon ($t\bar{t}\gamma$) is a direct probe of the top-photon electroweak coupling; a relatively unexplored property of the top quarks which is sensitive to new physics through several Beyond Standard Model (BSM) theories and top Effective Field Theory (EFT) coefficients, as discussed in Refs. [1–6].

The $t\bar{t}\gamma$ cross-section measurement presented here is based on the analysis in Ref. [7]. The measurement is performed using 20.2 fb^{-1} of data collected by the ATLAS detector [8] in the year 2012 at $\sqrt{s} = 8$ TeV.

* Presented at the Cracow Epiphany Conference on Advances in Heavy Flavour Physics, Kraków, Poland, January 9–12, 2018.

The cross section is measured within a fiducial volume, with a maximum-likelihood fit, using templates. The differential cross sections are measured within the same fiducial volume, in five bins of transverse momentum (p_{T}) and five bins of pseudorapidity (η) of the photon, and a bin-by-bin unfolding is applied.

The considered final state is the single lepton channel, where one of the W bosons decays into a lepton and a neutrino, and the other one into hadrons. Photons can originate not only from the top quarks, but also from the incoming partons and the charged particles in the decay chain of a $t\bar{t}$ pair. Example Feynman diagrams can be seen in Fig. 1. The event selection enhances γ radiation from top quarks.

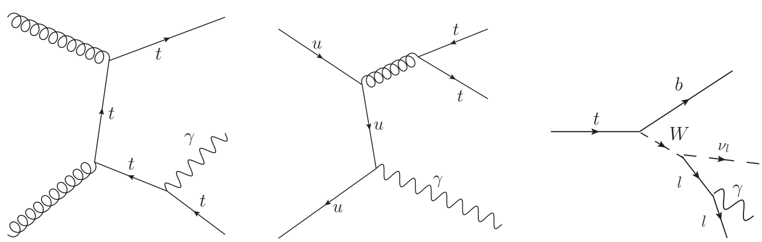

(a) (b) (c)

Fig. 1. Example Feynman diagrams for the $t\bar{t}\gamma$ process where the photon is radiated from a top quark (a), or from an initial parton (b) or from one of the decay products (c).

2. Analysis

The event selection is done by requiring exactly one electron or muon with $p_{\mathrm{T}} > 25$ GeV on which the event is triggered, at least four jets with $p_{\mathrm{T}} > 25$ GeV, where at least one of them is tagged as a b-jet, missing transverse momentum ($E_{\mathrm{T}}^{\mathrm{miss}}$) and the transverse mass of the W boson (m_{T}^{W}) to be $E_{\mathrm{T}}^{\mathrm{miss}} > 30$ GeV and $m_{\mathrm{T}}^{W} > 30$ GeV for the electron channel, and to be $E_{\mathrm{T}}^{\mathrm{miss}} > 20$ GeV and $E_{\mathrm{T}}^{\mathrm{miss}} + m_{\mathrm{T}}^{W} > 60$ GeV for the muon channel, exactly one photon with $p_{\mathrm{T}} > 15$ GeV and $|\eta| < 2.37$, an angular distance $\Delta R = \sqrt{(\Delta\eta)^2 + (\Delta\phi)^2}$ of greater than 0.5 between the photon and any jets and greater than 0.7 between the photon and the lepton, and the invariant mass of the photon and electron ($m_{e\gamma}$) to be outside of a 5 GeV mass window around the Z boson mass.

The fiducial region is defined for the Monte Carlo simulated events at particle level (*i.e.* before detector simulation) by cuts that mimic the event selection above, with the difference being that the cuts on $E_{\mathrm{T}}^{\mathrm{miss}}$, m_{T}^{W} and $m_{e\gamma}$ are not included, in order to have a common fiducial region for the electron and muon channel. The objects used in the fiducial region definition are constructed from the stable particles in the event record of the generator.

After the event selection, three category of events enter the signal region: (1) Events with prompt photons; this category includes the signal events and the background processes with a prompt photon; (2) Events with a photon originated from a hadron or a hadron misidentified as a photon, called *hadronic fake*; (3) Events with an electron misidentified as a photon, called *electron fake*.

The total and differential cross sections are extracted from a maximum-likelihood fit using three different templates, one for each of the category of events above. The discriminant variable used is the photon track isolation ($p_{\mathrm{T}}^{\mathrm{iso}}$), defined as the sum of p_{T} of the tracks within a cone of $\Delta R = 0.2$ around the photon.

The prompt-photon template is extracted from the $t\bar{t}\gamma$ signal Monte Carlo sample. After the full event selection is applied, the reconstructed photons that are geometrically matched to a particle level photon are used for the template.

The hadronic-fake template is extracted from a control region in data, enriched with the hadronic fakes. The control region is selected by requiring at least one photon which fails specific photon identification criteria, at least four jets, and $\Delta R(e,\gamma) > 0.1$. The differences of the p_{T} and η distributions of the hadronic fakes in the control region and the signal region are taken into account and the template is re-weighted accordingly. The prompt-photon contamination is taken into account as systematic uncertainty.

The electron-fake template is extracted from a control region in data, enriched by $Z \to e$+fake-γ events. The control region is selected by requiring a back-to-back $e\gamma$ pair with $m_{e\gamma}$ close to the Z boson mass, $p_{\mathrm{T}}^{e} > p_{\mathrm{T}}^{\gamma}$, and $E_{\mathrm{T}}^{\mathrm{miss}} > 30$ GeV. Backgrounds are subtracted using a sideband fit to the $m_{e\gamma}$ distribution.

The three templates for the inclusive cross-section measurement are shown in Fig. 2. For the differential cross-section measurements, all three templates are extracted for each of the p_{T} and η bins.

The largest background contribution comes from the events with hadronic fakes. This background is estimated from data using the template fit, by keeping the number of hadronic-fake background events a free parameter in the fit.

The second largest background is due to the events with an electron fake. This background is estimated from data. The ratio of the number of $Z \to e+$fake-γ events to the number of $Z \to ee$ is calculated as the function of p_{T} and η of photons and taken as the fake rate. Then the fake rates are applied to a modified signal region, where an electron is replacing the photon in the nominal $t\bar{t}\gamma$ selection.

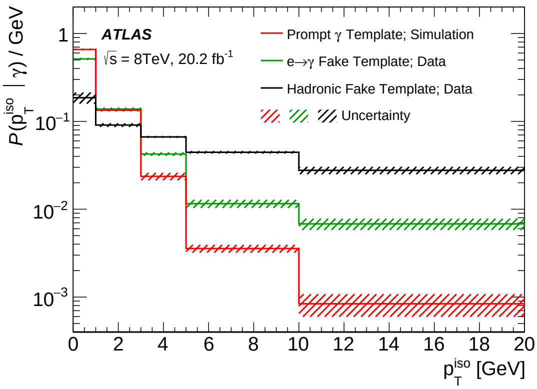

Fig. 2. The templates for the inclusive cross-section measurement for prompt photons, hadronic fakes and the fake photons from electrons [7]. The distributions are normalised to unity and the last bins contain the overflows. The dashed bands show the total uncertainty in each template.

Smaller background contributions come from the processes with a prompt photon. The multijet production with an associated prompt photon can be a background to $t\bar{t}\gamma$ when one of the jets is misidentified as a lepton. This background is estimated from data, using the matrix method. For the $W\gamma$+jets background, the Monte Carlo estimation is normalised by the data-driven scale factor, calculated from a dedicated control region. The rest, which are $Z\gamma$+jets, single top quark, and diboson productions with an associated prompt photon, are estimated from Monte Carlo simulations.

The likelihood fit function employed on the observed binned $p_{\mathrm{T}}^{\mathrm{iso}}$ distribution is defined as

$$\mathcal{L} = \prod_{i,j} P\left(N_{i,j}|N_{i,j}^{\mathrm{s}} + \sum_b N_{i,j}^{\mathrm{b}}\right) \cdot \prod_t G(0|\theta_t, 1)\,, \tag{1}$$

where j denotes the bins of $p_{\mathrm{T}}^{\mathrm{iso}}$ distribution and i denotes the bins of $p_{\mathrm{T}}(\eta)$ of photon in the differential cross-section measurement. In the Poisson function, $N_{i,j}$ is the observed number of events, while $N_{i,j}^{\mathrm{s}}$ and $N_{i,j}^{\mathrm{b}}$ are the expected numbers of signal and background events, respectively. The Gaussian function models the systematic uncertainty t, where θ_t is the parametrisation of this uncertainty.

There are two free parameters in the fit: number of signal events and number of hadronic fake background. The rest of the backgrounds are fixed in the fit, to their corresponding estimated number of events.

The fiducial and differential cross sections, σ_i, are related to the number of signal events by

$$N^s_{i,j} = L\,\sigma_i\,C_i\,f_{i,j}\,, \tag{2}$$

where L is the integrated luminosity, $f_{i,j}$ is the fraction of signal events falling into bin j of $p_{\mathrm{T}}^{\mathrm{iso}}$ of bin i of $p_{\mathrm{T}}(\eta)$, and C_i is the ratio of the number of reconstructed events to the number of generated events in the fiducial region in bin i. The ratio C_i corrects for the event selection efficiency and the migration of events between the fiducial and the non-fiducial region, or, in the case of differential cross-section measurement, between different i bins. This means the differential cross-section measurements are computed in each bin i with a bin-by-bin unfolding to the particle level.

Events from electron and muon channels are merged together and σ_i is the common parameter of interest in the maximum-likelihood fit.

3. Results

The fiducial cross section times the branching ratio is measured to be

$$\sigma_{\mathrm{sl}}^{\mathrm{fidu}} = 139 \pm 7(\mathrm{stat.}) \pm 17(\mathrm{syst.})\ \mathrm{fb} = 139 \pm 18\ \mathrm{fb}\,.$$

In Fig. 3, this result is compared to the Standard Model prediction at NLO accuracy [10] and to the previous measurement performed by ATLAS at $\sqrt{s} = 7$ TeV [9]. A good agreement between the measurement and the theory prediction is observed within the uncertainties.

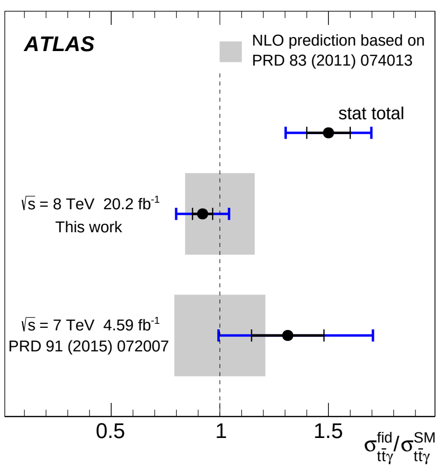

Fig. 3. Summary of $t\bar{t}\gamma$ fiducial cross-section measurements in pp collisions at $\sqrt{s} = 7$ TeV [9] and $\sqrt{s} = 8$ TeV [7], normalised to the expected cross section at NLO [10].

The most important systematic uncertainties in the fiducial cross-section measurement are listed in Table I, together with the statistical and the total uncertainty.

TABLE I

List of the most important systematic uncertainties and their effects on the measurement of the fiducial cross section, together with the statistical and the total uncertainty.

Source	Relative uncertainty [%]
Hadron-fake template	6.3
$e \to \gamma$ fake	6.3
Jet energy scale	4.9
$W\gamma$+jets	4.0
$Z\gamma$+jets	2.8
Initial- and final-state radiation	2.2
Luminosity	2.1
Statistical uncertainty	5.1
Total uncertainty	13

In addition, the results of the first differential cross-section measurements of $t\bar{t}\gamma$ are shown in Fig. 4, for five bins of p_{T} and five bins of η of the photons. The migration between the individual bins is found to be smaller than 7% and a bin-by-bin unfolding is applied. The comparison with the NLO theory prediction shows a good agreement within the uncertainties.

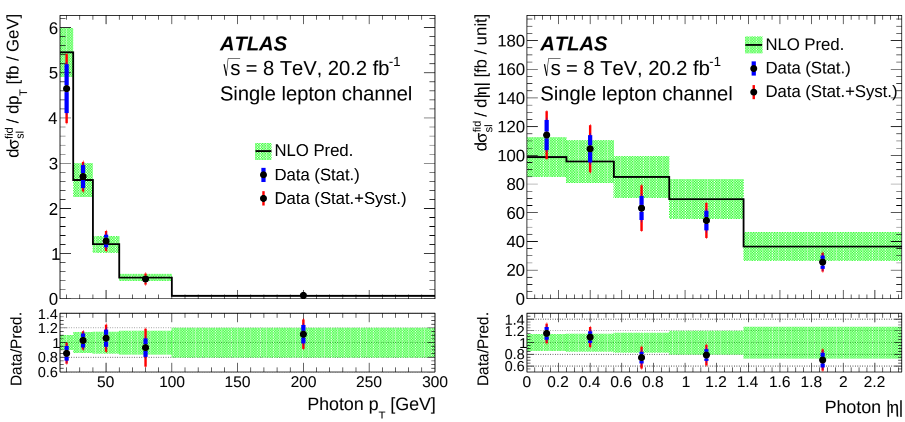

Fig. 4. Measured $t\bar{t}\gamma$ differential cross section in terms of photon p_{T} (left) and $|\eta|$ (right) and their theoretical prediction [7].

REFERENCES

[1] U. Baur, A. Juste, L.H. Orr, D. Rainwater, *Phys. Rev. D* **71**, 054013 (2005) [arXiv:hep-ph/0412021].

[2] A.O. Bouzas, F. Larios, *Phys. Rev. D* **87**, 074015 (2013) [arXiv:1212.6575 [hep-ph]].

[3] R. Röntsch, M. Schulze, *J. High Energy Phys.* **1508**, 044 (2015) [arXiv:1501.05939 [hep-ph]].

[4] M. Schulze, Y. Soreq, *Eur. Phys. J. C* **76**, 466 (2016) [arXiv:1603.08911 [hep-ph]].

[5] O. Bessidskaia Bylund *et al.*, *J. High Energy Phys.* **1605**, 052 (2016) [arXiv:1601.08193 [hep-ph]].

[6] P.-F. Duan *et al.*, *Phys. Lett. B* **766**, 102 (2017) [arXiv:1612.00248 [hep-ph]].

[7] ATLAS Collaboration, *J. High Energy Phys.* **1711**, 086 (2017) [arXiv:1706.03046 [hep-ex]].

[8] ATLAS Collaboration, *JINST* **3**, S08003 (2008).

[9] ATLAS Collaboration, *Phys. Rev. D* **91**, 072007 (2015) [arXiv:1502.00586 [hep-ex]].

[10] K. Melnikov, M. Schulze, A. Scharf, *Phys. Rev. D* **83**, 074013 (2011) [arXiv:1102.1967 [hep-ph]]. We thank the authors for repeating the calculation at $\sqrt{s} = 8$ TeV.